GA-A--20100

DE91 002706

SPECTROSCOPIC STUDY OF EDGE POLOIDAL ROTATION AND RADIAL ELECTRIC FIELDS IN THE DIII–D TOKAMAK

by

R.J. GROEBNER, K.H. BURRELL,
P. GOHIL, and R.P. SERAYDARIAN

This is a preprint of an invited paper to be presented at the 8th Topical Conference on High Temperature Plasma Diagnostics, May 7-10, 1990, Hyannis, Massachusetts, and to be printed in the *Proceedings*.

Work supported by
Department of Energy
Contract DE-AC03-89ER51114

GENERAL ATOMICS PROJECT 3466
OCTOBER 1990

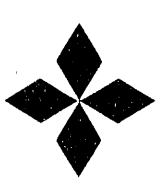

GENERAL ATOMICS

Spectroscopic study of edge poloidal rotation and radial electric fields in the DIII–D tokamak

R.J. GROEBNER, K.H. BURRELL, P. GOHIL,
AND R.P. SERAYDARIAN

General Atomics, San Diego, California 92186-9084

Doppler-shift spectroscopy has shown that finite values of poloidal rotation velocity v_θ and of radial electric field E_r exist at the edge of a tokamak plasma and that dramatic increases occur in these parameters at an L-H transition. E_r is negative in the L–mode and becomes more negative in the H–mode; v_θ increases in magnitude at the transition. In addition, the radial gradients (shear) of v_θ and E_r are large and these gradients also increase at the L-H transition. These results are based on measurements of Doppler shifts of light emitted by He II ions, located in a region about 1-3 cm inside the separatrix. These observations have been made with horizontally-viewing and vertically-viewing spectrometer systems on the DIII–D tokamak. The nearly orthogonal views of these systems are used to determine the plasma's flow velocity in terms of the orthogonal sets v_θ and v_ϕ or of $v_\perp$ and $v_\parallel$. Knowledge of $v_\perp$ is used to calculate E_r from the force balance equation for a single ion species. The existing results impose constraints on theories of the L-H transition. More detailed studies of the spatial profiles and temporal evolution of v_θ and E_r will be made with upgraded instrumentation, which is now coming on-line.

INTRODUCTION

Obtaining an understanding of the cause of the transition from L–mode to H–mode confinement[1–4] is a key issue facing the tokamak community. The H–mode discharge develops spontaneously from the L–mode discharge and has significantly better confinement properties than the L–mode. A theoretical understanding of the cause of the transition could lead to further improvements in confinement in present day tokamaks and to improvements in the design of the next generation of tokamaks, which need confinement comparable to that of the H–mode to reach their objectives. Recent theoretical work has suggested a link between the L-H transition and changes in the plasma's radial electric field E_r.[5–8] Subsequently, it has been discovered in the DIII–D tokamak that dramatic changes in the poloidal rotation velocity v_θ and in the radial electric field E_r occur at the plasma edge at the L-H transition.[9,10] E_r is found to be negative in the L–mode and to become more negative in the H–mode, as predicted by Shaing and coworkers.[7,8] Motivated by these experimental observations, Shaing and Crume have refined their model,[11] which shows that ion orbit loss produces a torque which drives poloidal rotation. Biglari, Diamond and Terry have proposed that shear in the profile of v_θ may play a role in causing the L-H transition.[12] (In the context of this paper, shear refers to the radial gradient of v_θ or of E_r.) The key features of these newer theories are consistent with the experimental observations of v_θ and E_r in the DIII–D tokamak.[13] Thus, there is strong evidence that E_r and v_θ play a crucial role in the L-H transition, and on-going theoretical and experimental studies may ultimately lead to a deep understanding of the transition. This point of view has been strengthened by a recent experiment in the CCT tokamak in which the

H–mode transition was induced with an internal electrode used to impose a radial electric field on the plasma.[14]

This paper discusses the techniques used to measure v_θ and E_r in the DIII–D tokamak. Doppler spectroscopy is used to measure the components of the plasmas's flow velocity within a flux surface. These measurements allow a determination of v_θ and also of $v_\perp$, the component of rotation perpendicular to the total magnetic field. The $\vec{V} \times \vec{B}$ component of E_r is calculated by using the lowest order force balance equation, which relates $v_\perp$ to E_r and to the gradient of the ion pressure.

Other diagnostics which have been used to measure E_r in a tokamak include electrostatic probes[14,15] and a heavy ion beam probe.[16] These diagnostics measure the plasma potential directly and the radial electric field is obtained from profile measurements of the plasma potential. In machines with auxiliary-heating, the use of probes is generally restricted to that region of the plasma which lies outside the last closed flux surface. Insertion of the probe past that flux surface leads to destruction of the probe by the plasma unless the probe is inserted and withdrawn rapidly by an appropriate reciprocating mechanism. Such a probe will be installed on the DIII–D tokamak at a future date. The heavy ion beam probe is used to make measurements in the main body of the plasma. This diagnostic is not available on the DIII–D tokamak. Work on the ISX-A tokamak in which both measurements of the toroidal rotation velocity profile v_ϕ from Doppler-shift spectroscopy and measurements of the plasma potential from a heavy ion beam probe were available found that the two techniques for measuring E_r obtained the same qualitative trends as the plasma parameters were changed. The quantitative results from the two diagnostics agreed within error

bars, which were large due to experimental uncertainties.[16-17] The work on ISX was performed for the main body of the discharge for which v_θ was thought to be small. The work reported in this paper is for the plasma periphery for which v_θ has been found to be large and non-negligible.

This paper is divided into three sections. The first section discusses the instrumentation and spectral analysis techniques used in the rotation measurements. Section II presents the techniques used to obtain the rotation velocities and the radial electric field and presents some results. The rotation measurements discussed in this section were obtained from emission spectroscopy. Section III is a brief discussion of an upgrade to the instrumentation designed to look at the plasma edge in great detail via the techniques of charge exchange recombination (CER) spectroscopy. Initial results from this instrumentation will be presented. A summary is presented in Section IV.

I. EXPERIMENTAL APPARATUS

The Doppler-shift measurements have been made with the two 8-chord spectrometer systems designed to measure the ion temperature T_i, v_ϕ and v_θ profiles on the DIII–D tokamak.[18] These instruments are very similar to the multi-chord spectrometer system used for T_i and v_ϕ measurements on the DIII tokamak.[19] Light is transmitted from the plasma to the spectrometers by ≈8–10 m lengths of 1500 micron core diameter quartz fiberoptics. The detectors consist of dual-stage microchannel plate image intensifiers which are fiber- optically coupled to linear photodiode arrays. The electronics permit integration times as short as 2 ms and 250 data frames are

obtained per discharge with memory requirements of 62.5K words per spatial chord. The data are digitized with 12-bit resolution. Ruled gratings with line spacings of 1200 g/mm and 1800 g/mm have been used on 3/4-m and 1-m Czerny-Turner spectrometers. With each pixel being 25 microns wide, the reciprocal linear dispersion is in the range 0.13 to 0.28 Angstroms/pixel.

Several steps are taken to insure the highest possible quality of the data. After each plasma discharge, six background spectra, consisting of dark current and fixed-pattern readout noise, are obtained and stored for each chord. These spectra are averaged and subtracted from the data at the time of analysis. Furthermore, to account for differences in gain between pixels, a white light calibration is periodically performed and an appropriate gain factor is applied to the signal from each pixel. The instrumental profile for each chord is obtained by illuminating the input end of the fiberoptics with a low pressure mercury discharge lamp. The spectrum of the 546.05 nm line of Hg is obtained and fit with a function which is the sum of three Gaussians. This type of modelling fits the instrumental profile to a high degree of accuracy. Actual analysis of plasma data is performed by doing a non-linear least squares fit to the convolution of a Gaussian with the instrumental profile. The fitting algorithm is discussed at length in Ref. 19.

One of the spectrometer systems views the plasma horizontally and the other nearly vertically, as illustrated in Fig. 1. With these nearly orthogonal systems, the plasma flow velocity can be determined in terms of the orthogonal sets v_θ and v_ϕ or of $v_\perp$ and $v_\parallel$, where $v_\parallel$ is the component of rotation parallel to the total magnetic field. These instruments are oriented so that their lines of sight cross the paths of

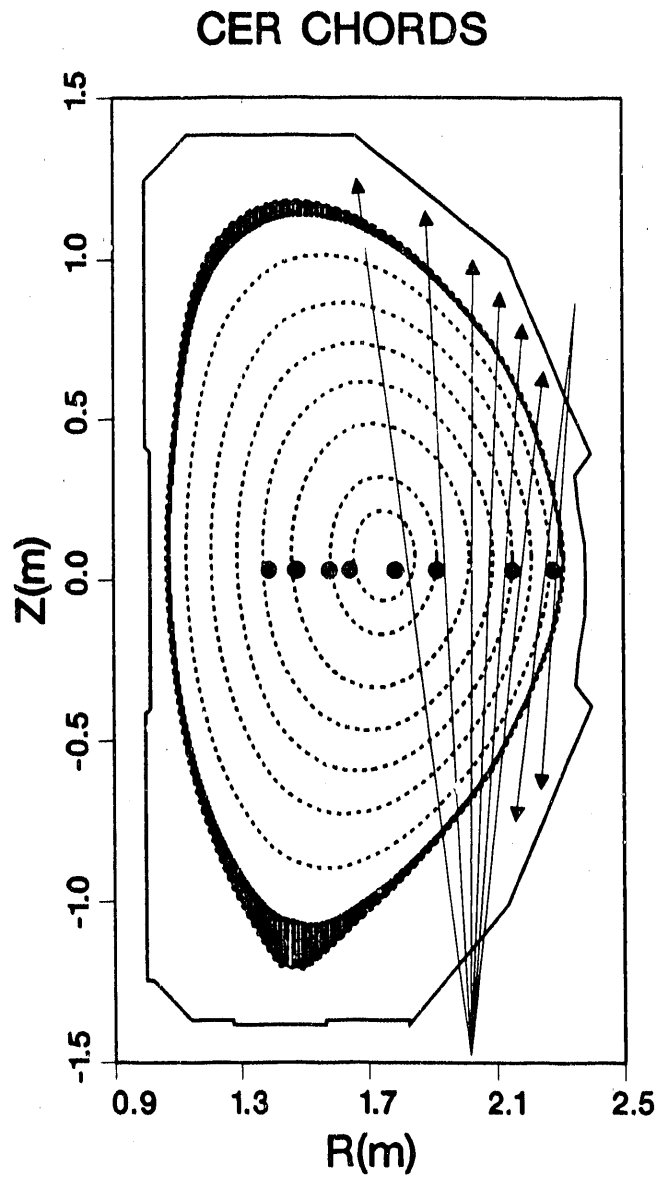

Fig. 1. CER view chords projected onto a typical H–mode equilibrium. Six chords view vertically upwards, two chords view vertically downwards and eight chords view horizontally (out of the paper). Emission from the He II warm component at 468.6 nm is emitted from a narrow region inside the separatrix, as indicated by shaded area. B_{T} points out of the paper, I_{p} points into the paper and beam injection is in the direction of I_{p}.

neutral beams, in order to measure T_i and v_ϕ profiles via the techniques of CER spectroscopy.[20] However, for most of the work discussed here, the beams required for CER measurements have not been turned on, and the He II line at 468.6 nm has been viewed in emission only.

In the absence of neutral beam excitation, the He II spectrum is composed of two components, the "cold" peak, which has T_i of 20–40 eV and is located at or outside the plasma edge, and the "warm" peak, which has T_i of 100–1000 eV. The cold peak is the emission line expected as He^+ ions drift into the plasma and are ionized by collisions with electrons with temperatures comparable to the 54.4 eV ionization potential of He^+. The warm line, which was first identified in the JET tokamak,[21,22] is observed at temperatures where He is expected to be fully ionized and incapable of radiating line emission. However, neutral D° or He° atoms can penetrate a short distance into the plasma, and very near the plasma periphery it is likely that these atoms undergo charge transfer reactions with He^{++}. The resulting He^+ ions are left in excited states and some of them radiate at 468.6 nm, due to the He II 4-3 transition. A warm line has also been observed for the D° line at 656.1 nm, presumably produced by the same process. Charge transfer between intrinsic neutral hydrogen and low charge states of oxygen has been observed in the ISX-A tokamak,[23] and charge transfer between intrinsic neutral hydrogen and injected Argon ions has been studied in the Alcator-C tokamak.[24,25]

The warm He^+ component is routinely observed in ohmically-heated and auxiliary-heated discharges in the DIII–D tokamak. The ratio of the intensities of

the warm to cold components is typically about 1 to 3. Helium is an intrinsic component of discharges in DIII–D, because glow discharge cleaning in helium is routinely done between discharges. The concentration of helium is estimated to be a few percent of the electron density, and the intensity of the two He components is sufficiently large that the detectors are operated very far from the limit of single photoelectron detection. Thus, the signal quality is generally very good, and this is a key ingredient in being able to unambiguously observe poloidal rotation and to observe relatively small changes in v_θ and $v_\perp$.

The emitting regions for the warm and cold helium components are obtained in two ways. The fact that the lines are observed on all of the CER chords indicates that they are emitted from a region outside that observed by the outermost chord, which is nominally 2–4 cm from the plasma edge. A better determination of location is obtained by comparing the measured T_i with the electron temperature T_e profile, obtained from a multipoint Thomson scattering system. With the assumption that T_i and T_e are roughly equal near the plasma edge, it is found that the warm component is always emitted from a region about 1 to 3 cm inside the separatrix, and the cold component is emitted from very near the separatrix. The assumption that $T_i = T_e$ near the plasma edge is supported by comparisons of T_i profiles from CER data and T_e from Thomson scattering and by the fact that the equilibration time between ions and electrons is only a few milliseconds due to the high densities and low temperatures near the separatrix.

As an example, Fig. 2 shows the electron density n_e and T_e profiles near the plasma edge for a typical H–mode discharge. These profiles have very steep gradients

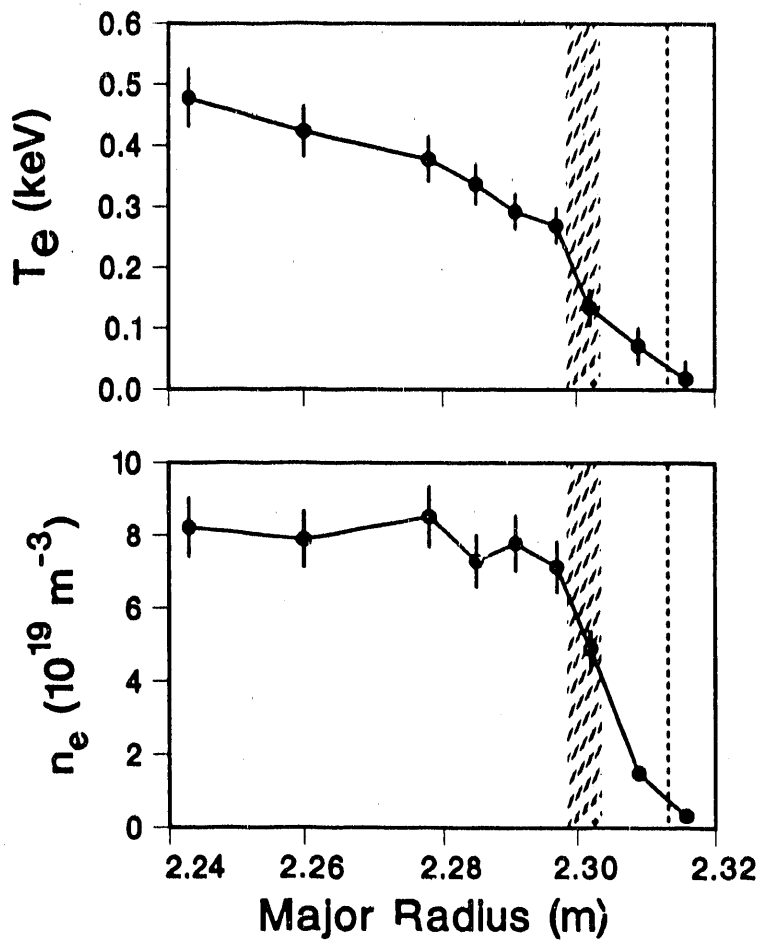

Fig. 2. T_e and n_e profiles obtained from multipoint Thomson scattering system are shown in a) and b) respectively. Location of separatrix is shown by dashed line. Warm peak had a temperature of 0.15 keV and was located at major radius of about 2.30 m under assumption that $T_i = T_e$. Cross hatched shows region of emission with assumption that emitting region was 0.5 cm thick.

inside the separatrix (located at 2.313 m) with scale lengths of about 2 cm. At the time that the Thomson data were obtained, the warm He^+ peak had a temperature of 0.15 keV. Under the assumption that $T_i = T_e$, the location of this emission was at a major radius of 2.31 cm, which was about 1–1.5 cm inside the separatrix. The cold peak with a temperature of about 20 eV was emitted from very near the separatrix.

As is the typical case, the warm peak emission came primarily from the region of the density gradient at the plasma edge. This location is consistent with the notion that thermal neutrals penetrate a short distance into the plasma and produce the warm peak by the process of charge transfer with fully ionized He. The width of the emitting region for the warm peak has not been measured. However, the warm and cold peaks are each fit well with single Gaussians, indicating that the emission is well localized in the steep temperature gradient region of the edge. The shaded region in Fig. 2 shows schematically the emission region of a 0.5 cm wide shell, centered at a temperature of 0.150 kV.

A series of Thomson profiles obtained during the evolution from L–mode to H–mode shows that the emitting region moves by no more than 1 cm. This result is equivalent to the fact that thermal neutrals cannot penetrate far into the plasma. Because the inferred location of the warm and cold components changes very little at the time of the transition, changes in the observed values of $v_\perp$ and v_θ at the L-H transition are interpreted as being due primarily to increases in the local values of $v_\perp$ and v_θ at fixed locations near the plasma periphery rather than to movement of the He II emission layer to regions of higher v_θ and E_r.

II. MEASUREMENT OF v_θ AND E_r

Under the assumption that the plasma flow lies in a flux surface, the rotation velocity $\vec{v}$ can be decomposed either as $\vec{v} = v_\theta\, \hat{e_\theta} + v_\phi\, \hat{e_\phi}$, where $\hat{e_\theta}$ and $\hat{e_\phi}$ are respectively unit vectors in the direction of the poloidal magnetic field and of the toroidal

magnetic field or as $\vec{v} = v_{\|}\,\hat{e_{\|}} + v_{\perp}\,\hat{e_{\perp}}$, where $\hat{e_{\|}}$ and $\hat{e_{\perp}}$ are respectively unit vectors parallel to and perpendicular to the total magnetic field. With knowledge of the viewing geometry and of the magnetic field structure, it is possible to calculate any of the components of rotation of the He II ions. Viewing geometry must be taken into account because due to the locations of diagnostic and neutral beam ports on the DIII–D vacuum vessel, it was necessary that the vertically-viewing chords be given some tilt in the toroidal direction so that these chords can view a neutral beam. Thus, poloidal or toroidal rotation can produce Doppler shifts on the vertical chords. Measurements of v_{ϕ} with the horizontal system are then required to remove the contribution of v_{ϕ} from the vertical data to obtain the poloidal rotation. The components of the magnetic field are calculated with the magnetics-analysis code EFIT.[26] Near the plasma periphery, the poloidal magnetic field can be calculated with a high degree of accuracy because nearly all of the plasma current is enclosed by flux surfaces near the plasma edge.

For a magnetically-confined plasma, the radial electric field is related to the plasma's flow velocity by the lowest order force balance equation for a single ion species[27]

$$E_r = \frac{1}{n_i\, Z_i e} \nabla \mathrm{P_i} - (\vec{\mathrm{V}}_i \times \vec{\mathrm{B}})_r \quad , \tag{1}$$

where n is ion density, Z is the ion charge, e is the electronic charge, P is the ion pressure, $\vec{\mathrm{V}}$ is the ion fluid flow velocity, $\vec{\mathrm{B}}$ is the total magnetic field, and i labels the ion species. The only component of $\vec{\mathrm{V}}_i$ which contributes to the radial component of

Eq. (1) is $v_\perp$. Thus, with measurements of $v_\perp$ obtained as described previously, the $\vec{V} \times \vec{B}$ contribution to the radial electric field can be calculated. For typical discharges in the DIII–D tokamak, $v_\perp$ for the warm component is typically in the range of 0–10 km/s in the L–mode and 15–30 km/s in the H–mode. The observed values of $v_\perp$ imply that the $\vec{V} \times \vec{B}$ term of Eq. (1) changes from typically 0–10 kV/m in the L–mode to 20–40 kV/m in the H–mode. For discharges with the toroidal field B_T in the standard direction, which is clockwise as viewed from the top of the tokamak, $v_\perp$ is directed up at the outside edge of the plasma. This geometry implies that the $\vec{V} \times \vec{B}$ term of Eq. (1) makes a negative contribution to E_r. Measurements of the ∇P_i term in Eqn (1) are not yet available. However, the sign of the ∇P_i term is also negative; thus the total E_r is definitely negative. Estimates of the magnitude of this term have been made from the electron pressure profile and the assumption that $P_i = P_e$. The ∇P_i term is estimated to have a magnitude of up to 20%–30% of the $\vec{V} \times \vec{B}$ term. The experimental values for E_r quoted in this paper are only the $\vec{V} \times \vec{B}$ term of Eq. (1) and their magnitude provides a lower limit for the true magnitude of E_r.

For fairly standard discharge conditions with $B_T = 1.5$–2.1 T and $I_p = 1.5$ MA, the magnetic field pitch is such that the edgemost vertical chord is in fact almost exactly perpendicular to the total magnetic field. This chord then measures $v_\perp$ with very high accuracy. By suitably correcting for toroidal rotation, it is found that the values of v_θ are comparable to those of $v_\perp$ in the L–mode and in the H–mode. Furthermore, the corrections for v_ϕ are typically small and the accuracy of the v_θ measurement is quite good.

An example of the Doppler shift of the He II warm line due to poloidal rotation is shown in Fig. 3, which shows spectra of the He II 468.6 nm line in the L–mode and H–mode phases of an NBI-heated discharge. Each spectrum is a superposition of the cold and warm components. A significant Doppler-shift of the spectrum from the L–mode to the H–mode is due to the increase in v_θ of the warm peak. The broadening of the spectrum is due to an increase in temperature of the warm component. The intensity of the peak of the spectra is due primarily to the cold component; the cold component shows little change in rotation across the L-H transition.

A time-resolved view of v_θ and E_r for the warm and cold components is shown for a typical L-H transition in Fig. 4. The abrupt drop in D_α emission, which occurred at 2194 ms, is the standard signature of the transition. E_r and v_θ change abruptly in magnitude within less than an integration period (2 ms) and then show a more gradual evolution which lasts for about 25 ms. The gradual evolution is highly correlated with the evolution time of the edge profiles, particularly changes in the ion temperature of the warm peak. Figure 4 also demonstrates that the cold and warm peaks have different values of E_r and v_θ. These peaks are separated by 1-3 cm and thus show that there is significant shear in the profiles of E_r and v_θ very near the plasma periphery. Furthermore, this shear increases from the L– to the H–mode.

An effort has been made to see how far into the plasma the large values of v_θ extend. These measurements have been made with the appropriate neutral beam turned on to permit measurements of the He II spectrum via CER spectroscopy. The available v_ϕ profiles are not sufficiently detailed to provide an answer with high confidence, but the Doppler shifts observed on the vertical chords a few cm inside the

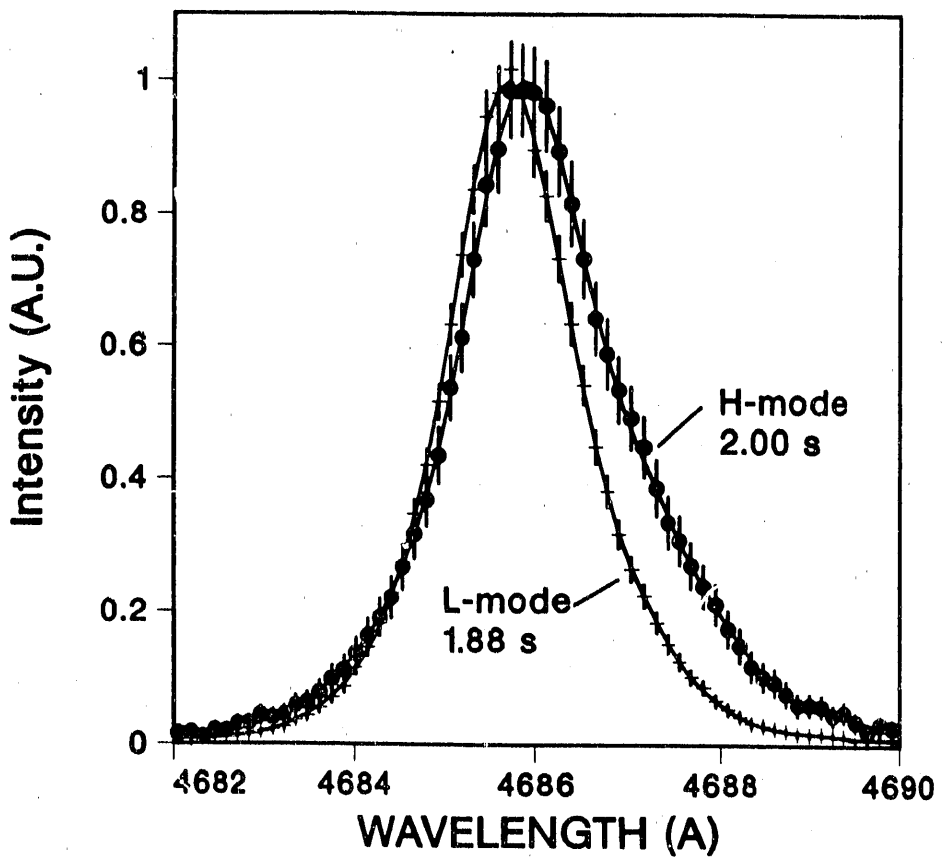

Fig. 3. He II spectra shown for L–mode and H–mode. H–mode spectrum from a downwards-viewing chord shows substantial red shift due to poloidal rotation of warm component in H–mode. Data were obtained with B_T direction opposite to that of normal setting. Peak of the emission is dominated by the cold component and shows little change from L–mode to H–mode. Peak intensity of both spectra have been normalized. Absolute intensity decreases by factor of 2-3 in H–mode relative to L–mode.

separatrix appear to be due primarily to toroidal rotation. Thus, the available data suggest the v_θ is peaked very near the plasma edge. Confirmation of this indication awaits data from the improved instrumentation discussed below.

If the v_θ profile is peaked and localized very near the plasma edge, then the warm peak emission is fortuitously emitted from that region of the plasma which exhibits the interesting values and behavior of v_θ discussed here. However, if v_θ is

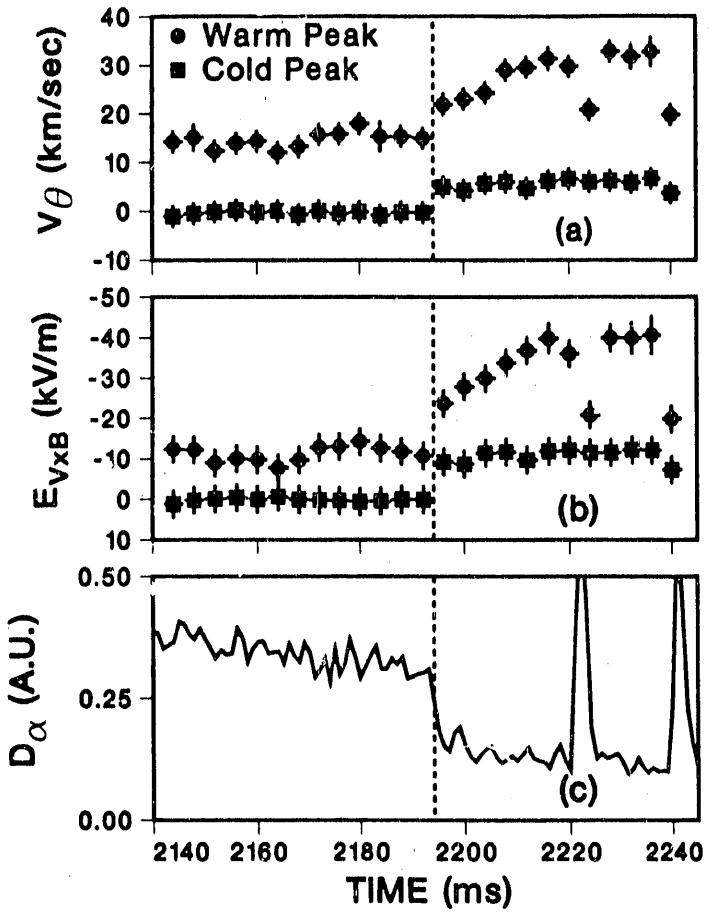

Fig. 4. T_i, v_θ and E_r from $\vec{V} \times \vec{B}$ term for warm and cold components shown respectively in (a), (b) and (c). D_α (d) shows that L-H transition occurred at 2192 ms, as indicated by dashed line, and shows that large ELMs occurred at 2220 and 2240 ms.

highly peaked and if the He II emission region is highly localized, then inferences from the measurements of the warm peak could lead to some confusion depending on exactly where on the v_θ profile the light from the warm peak is emitted. For example, discharges have been studied in which the values of v_θ and E_r obtained from the warm peak show increases in magnitude 5-10 milliseconds prior to the L-H transition.[13] Such observations suggest that changes in v_θ or E_r cause the L-H transition. However, as shown in Fig. 4, there are many discharges in which no changes are observed prior

to the transition; rather v_θ and E_r increase abruptly at the transition. One possible unifying explanation for these contradictory observations is that precursors do occur in E_r and v_θ but that these changes are localized to a very small region, possibly on the order of a few millimeters. Because the layer of warm peak emission is controlled by atomic physics processes, sometimes the He II emission comes from the appropriate region and sometimes the He II emission comes primarily from a neighboring region and does not show the precursor activity. Another possible explanation which relies on the fact that v_θ and E_r change very rapidly in space is that due to changes in the edge density and temperature profiles, the He II emission region might move a few millimeters into regions of increased E_r and v_θ prior to the transition. Resolution of these issues awaits measurements from the upgraded instrumentation. These issues are important because at least two theories of the L-H transition imply that changes in v_θ and E_r should occur prior to the transition.[11,12]

This section will be concluded with a discussion of potential systematic errors which could produce spurious shifts of the He II components. The error bars for rotation velocities shown in the figures are based on the statistics of the fit under the asumption that the uncertainties in the measurements are due to photon statistics. However, effects such as contamination of the spectra from weak impurity lines, difficulties in accurately fitting multiple Gaussians to the data, and pixel-to-pixel gain variations could produce small errors in the locations of the fitted peak locations. Due to the care taken to fit the data as accurately as possible and to the very strong signals from the He emission lines, potential errors due to these effects are not nearly large enough to account for the observed values of $v_\perp$ and v_θ in the H–mode. Furthermore,

various features of the data defy explanation by systematic errors. For example, the downwards-viewing chords observe blue shifts when the upwards-viewing chords observe red shifts. Also, Eqn. 1 would predict that $v_\perp$ should reverse direction if the magnetic field direction is reversed, a prediction which has been verified by reversing the direction of the toroidal field. In this case, the downwards-viewing chords observe red shifts while the upwards-viewing chords observe blue shifts. Finally, for the geometry of the chords as shown in Fig. 1, the observed Doppler shifts on the vertical chords should decrease monotonically for chords which view at smaller major radii. One reason for this is that projection of v_θ into the viewing direction decreases monotonically from the edgemost to the innermost chord. A second reason is that for the product of poloidal flow velocity and plasma area to be conserved, v_θ must decrease as the separation between flux surfaces increases. Figure 1 shows that the distance between two given flux surfaces is a minimum for the edgemost chord and increases monotonically in the direction of view of the innermost chords. Each of these effects should give roughly a factor of two reduction in the observed Doppler shift from the outermost to the innermost chord. The data do show a monotonic decrease in observed Doppler shifts from outermost to the innermost chord, as expected, and the decrease is of the magnitude expected. In summary, the data show all of the signatures expected from poloidal flows near the plasma boundary.

III. UPGRADED INSTRUMENTATION FOR EDGE STUDIES

Further studies of the physics of the L-H transition require detailed information regarding the spatial profiles and the temporal evolution of the profiles of v_θ and

E_r near the plasma boundary. For this purpose, the CER instrumentation has been upgraded with the addition of 8 vertically-viewing and 8 tangentially-viewing chords positioned to study the plasma edge.[28] Within each system, the chords are spaced 1.5 cm apart with a spatial resolution of about 0.5 cm per chord, and the vertically-viewing and horizontally-viewing positions are interleaved. These chords view a region spanning about 12 cm with the edge of the viewed region coinciding with the typical location of the separatrix. To obtain spatial profiles, these systems will view light produced by charge transfer between the appropriate neutral beam and ions in the plasma. Initial results indicate that the C VI 529.0 nm line is a good candidate in that the signal to background ratio is generally quite good. Low intensity lines due to either a cold line of C VI 529.0 or the O IV 529.0 nm line are also sometimes observed.

Figure 5 shows initial results from this system for a time range which spans an L-H transition. Figure 5(a) and 5(b) show respectively that T_i and v_ϕ are increasing at all spatial locations during the L phase and these increases continue into the H–phase. Figure 5(c) shows that the poloidal rotation profile is peaked very near the plasma periphery during the H–mode.

IV. SUMMARY

Studies of an emission line of He II have shown that finite values of v_θ and E_r exist at the edge of a tokamak discharge and that these values change dramatically during the L-H transition. Non-zero shear exists in the gradients of v_θ and E_r at the edge and this shear also increases at the L-H transition. These studies are leading to a deeper understanding of the physics of the L-H transition. The number of chords

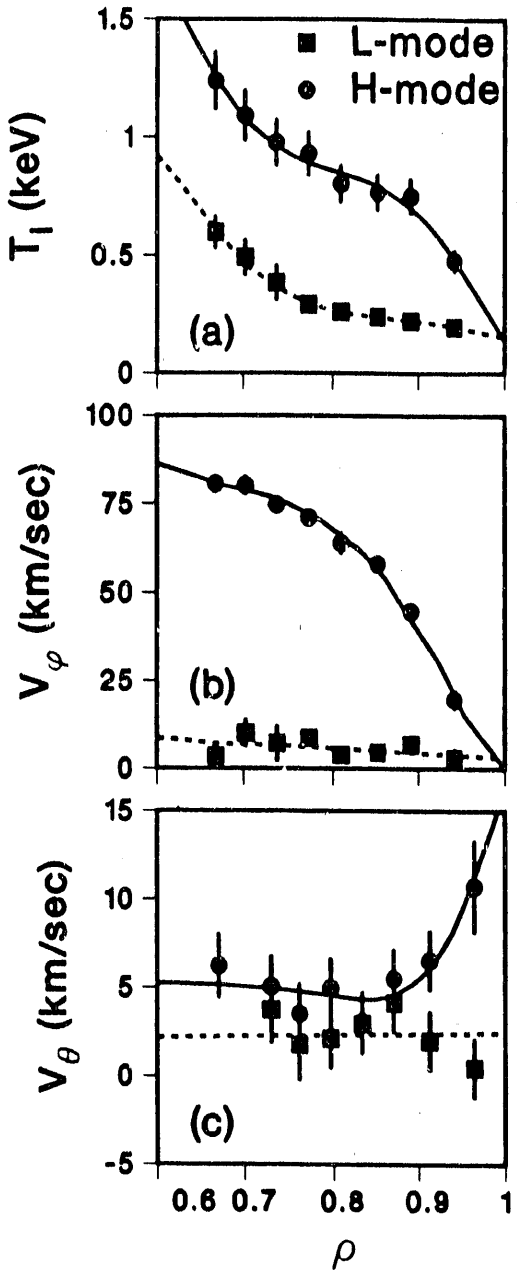

Fig. 5. Profiles of T_i, v_ϕ and v_θ shown in (a), (b) and (c) as functions of time for data obtained with upgraded CER instrumentation. Time of L-H transition shown by dashed line.

in the spectroscopic instrumentation has been increased by a factor of two with the new chords viewing the outer 10–12 cm of the discharge so that detailed information regarding the spatial profiles and temporal evolution of T_i, v_ϕ and v_θ can be obtained. This information is expected to lead to further advances in the understanding of the L-H transition.

ACKNOWLEDGMENTS

The authors acknowledge encouragement from T. Carlstrom, invaluable assistance with electronics from J. Haskovec and E. McKee and the general support of the DIII–D group. The continuing support of R. Stambaugh and T. Simonen is appreciated. This is a report of work sponsored by the U.S. Department of Energy under contract No. DE-AC03-89ER51114.

REFERENCES

[1] F. Wagner *et al.*, Phys. Rev. Lett. **49**, 1408 (1982).

[2] S. M. Kaye *et al.*, J. Nucl. Mater. **121** 115 (1984).

[3] K. H. Burrell *et al.*, Phys. Rev. Lett. **59**, 1432 (1987).

[4] A. Tanga *et al.*, Nucl. Fusion **27**, 1877 (1987).

[5] S. Itoh and K. Itoh, Phys. Rev. Lett. **60**, 2276 (1988).

[6] S.-I. Itoh and K. Itoh, Nucl. Fusion **29**, 1031 (1989).

[7] K. C. Shaing, W. A. Houlberg, and E. C. Crume, Comments Plasma Phys. Controlled Fusion **12**, 69 (1988).

[8] K. C. Shaing, G. S. Lee, B. A. Carreras, W. A. Houlberg and E. C. Crume, Jr., to be published in *Proceedings of the Twelfth International Conference on Plasma Physics and Controlled Nuclear Fusion Research*, Nice, 1988 (International Atomic Energy Agency, Vienna, 1989)

[9] R. J. Groebner, P. Gohil, K. H. Burrell, T.H. Osborne, R.P. Seraydarian, and H. St.John, in *Proceedings of the Sixteenth European Conference on Controlled Fusion and Plasma Physics, Venice, 1989* (European Physical Society, Petit-Lancy, Switzerland, 1989), Vol. **13B**, p. 245.

[10] K. H. Burrell *et al.*, Plasma Physics and Controlled Fusion **31**, 1649 (1989).

[11] K. C. Shaing and E. C. Crume, Jr., Phys. Rev. Lett. **63**, 2369 (1989).

[12] H. Biglari, P. H. Diamond, and P. W. Terry, Physics of Fluids B **2**, 1 (1989).

[13] R. J Groebner, K. H. Burrell and R. P. Seraydarian, General Atomic report GA-A19813 (1989), submitted to Phys. Rev. Lett.

[14] R. J. Taylor, *et al.*, Phys. Rev. Lett. **63**, 2365 (1989).

[15] C. P. Ritz, D. L. Brower, T.L. Rhodes, R. D. Bengston, S. J. Levinson, N. C. Luhmann, Jr., W. A. Peebles and E. J. Powers, Nucl. Fusion **27**, 1125 (1987).

[16] G. A. Hallock, J. Mathew, W. C. Jennings, R. L. Hickok, A. J. Wooton, and R. C. Isler, Phys. Rev. Lett. **56**, 1248 (1986).

[17] R. C. Isler, A. J. Wooton, L. E. Murray, R. A. Langley, J. D. Bell, C. E. Bush, *et al.*, Nucl. Fusion, **26**, 391 (1986).

[18] R. P. Seraydarian and K. H. Burrell, Rev. Sci. Instrum. **57**, 2012 (1986).

[19] R. P. Seraydarian, K. H. Burrell, N. H. Brooks, R. J. Groebner, and C. Kahn, Rev. Sci. Instrum. **57**, 155 (1986).

[20] R. J. Fonck, D. S. Darrow, and K. P. Jaehnig, Phys. Rev. A **29**, 3288 (1984).

[21] P. G. Carolan, M. J. Forrest, N. C. Hawkes, and N. J. Peacock, in *Proceedings of the Twelfth European Conference on Controlled Fusion and Plasma Physics, Budapest, 1985* (European Physical Society, 1985), Vol. 77, p. 263.

[22] A. Boileau, M. von Hellermann, L. D. Horton, J. Spence, and H. P. Summers, Plasma Physics and Controlled Fusion **31**, 779 (1989).

[23] R. C. Isler and E. C. Crume, Phys. Rev. Lett. **41**, 1296 (1978).

[24] E. Kallne, J. Kallne, A. Dalgarno, E. S. Marmar, J. E. Rice, and A. K. Pradhan, Phys. Rev. Lett. **52**, 2245 (1984).

[25] J. E. Rice, E. S. Marmar, J. L. Terry, E. Kallne, and J. Kallne, Phys. Rev. Lett. **56**, 50 (1985).

[26] L. Lao, H. St.John, R. D. Stambaugh, A. G. Kellman, W. Pfeiffer, Nucl. Fusion **25**, 1611 (1985).

[27] F. L. Hinton and R. D. Hazeltine, Rev. of Mod. Physics **48**, 239 (1976).

[28] P. Gohil et al., submitted to Rev. Sci. Instrum.

END

DATE FILMED

12/03/90